Proc. Natl. Acad. Sci. USA
Vol. 93, pp. 11640–11645, October 1996
Biophysics

Profluorescent protease substrates: Intramolecular dimers described by the exciton model

BEVERLY Z. PACKARD*, DMITRI D. TOPTYGIN†, AKIRA KOMORIYA*, AND LUDWIG BRAND†

*OncoImmunin, Inc., 335 Paint Branch Drive, College Park, MD 20742; and †Biology Department, Johns Hopkins University, 3400 North Charles Street, Baltimore, MD 21218

Communicated by Robin M. Hochstrasser, University of Pennsylvania, Philadelphia, PA, August 2, 1996 (received for review March 21, 1996)

ABSTRACT **Xanthene dyes are known to form dimers with spectral characteristics that have been interpreted in terms of exciton theory. A unique aspect of H-type dimers is the fluorescence quenching that accompanies their formation. Using the principles of exciton theory as a guide, a series of protease substrates was synthesized with a xanthene dye on each side of the cleavage site. To bring the attached dyes into spatial proximity to form a dimer, the molecular design included structure determinant regions in the amino acid sequence. In addition, chromophores were chosen such that changes in absorption spectra indicative of exciton splitting were anticipated. Cleavage of the peptides by a protease resulted in disruption of the dimers and indeed significant absorption spectral changes were observed. Furthermore, substrate cleavage was accompanied by at least an order of magnitude increase in fluorescence intensity. This has allowed determination of intracellular elastase activity using a fluorescence microscope equipped with standard optics.**

The molecular exciton represents a delocalized electronic excitation in a system of identical molecular units (1). Based on a resonance dipole–dipole interaction mechanism, exciton theory predicts and explains the spectroscopic characteristics in systems of interacting fluorophores. Although the original definition of excitons was introduced for molecular crystals (2), the same formalism can also be applied to explain spectra of other molecular aggregates such as monomolecular lamellar systems (3) as well as dye dimers (4, 5). The latter are usually classified as either H- or J-type aggregates depending on the spatial arrangement of the fluorophores and the resulting spectral characteristics (6). Xanthene dyes are known to form H-type dimers, the characteristics of which are a blue shift in the absorption spectrum and the loss of fluorescence (7–9).

If one were to design a functional molecular structure that fits the exciton model, one could have a reporter molecule with a unique self-contained analytical tool. We now report the design of a new class of profluorescent protease substrates. First, polypeptides containing amino acid sequences of naturally occurring protease inhibitors for protease recognition were synthesized; second, synthesis was followed by derivatization with a fluorophore on each side of the cleavage site. The size and geometry of the doubly labeled polypeptides are favorable for the formation of H-type dimers. Cleavage of such a polypeptide by a protease results in disruption of the H-type dimer and appearance of fluorescence.

MATERIALS AND METHODS

Materials. N^{α}-9-Fluorenylmethoxycarbonyl (Fmoc) amino acids were purchased from Calbiochem–Novabiochem. 2-Chlorotrityl resin was obtained from Peptides International. The coupling reagent benzotriazol-1-yl-oxy-tris-pyrrolidinophosphonium hexafluorophosphate (PyBOP) was bought from Advanced ChemTech. Solvents such as HPLC grade dichloromethane, methanol, and acetonitrile were from Fisher Scientific. Other reagents such as 1-methyl-pyrrolidinone (NMP), 4-methylmorpholine (NMM), 1-hydroxybenzotriazole, diisopropylethylamine, and protein sequencing grade trifluoroacetic acid (TFA) were from Aldrich. Fluorophores 5′,6′-carboxytetramethylrhodamine, succinimidyl ester and 5,6-carboxy-X-rhodamine, succinimidyl ester were from Molecular Probes, and porcine pancreatic elastase was from Sigma. A C_{18} reverse-phase HPLC column was from Vydac (Hesperia, CA). RPMI medium 1640 and fetal calf serum were from GIBCO.

Peptide Synthesis. Peptides were synthesized using manual Fmoc chemistry with PyBOP, HBOT, and NMM as coupling reagents in NMP. The molar excess of Fmoc amino acid used for each coupling step was 3-fold. Kaiser tests were performed after each coupling cycle to ensure completion of the reaction. Crude peptides as well as conjugated peptides were purified by reverse phase HPLC using a C_{18} column and a water/acetonitrile (containing 0.075% TFA) gradient. Final conjugated peptides were characterized by both amino acid composition (PICO-Tag) analysis and mass (MALDI-TOF) spectrometry using a Kratos Analytical Instruments model Kompact MALDI 1 time of flight mass spectrometer from Shimadzu. The matrix used was α-cyano-4-hydroxycinnamic acid and the mass calibration standards used were Leu-enkephalin, bradykinin, and melittin (566.6, 1061.2, and 2847.5 atomic mass units, respectively). Concentrations of substrates were determined by amino acid analysis.

Peptide Derivatization with Fluorophores. Peptides were sequentially derivatized with 5′,6′-carboxytetramethylrhodamine, succinimidyl ester and/or 5′,6′-carboxy-X-rhodamine, succinimidyl ester by dissolving the unlabeled partially deprotected peptide and probe at molar ratios of 1:1.5 in a minimal amount of an organic solvent such as NMP and diisopropylethylamine. By choosing the appropriate orthogonal protecting groups such as Fmoc and t-butyloxycarbonyl (t-Boc) for the α-amino group of aspartic acid and the ε-amino group of lysine, respectively, only one amino group per peptide was available for each fluorophore coupling step. After purification by reverse-phase HPLC, the singly labeled peptides were covalently coupled to the second fluorophore by a similar procedure. The doubly labeled peptides were then also purified by reverse-phase HPLC. The two fluorophore isomers, i.e., the 5′-carboxyl and 6′-carboxyl fluorophore-derived peptides, were separated at each step during the purification. Molecular weights were determined by mass spectrometry.

Digestion of Peptides with Elastase. Enzymatic digestion of peptides (4×10^{-7} M) and elastase (0.5 unit/ml) was carried out in a buffer composed of 50 mM Tris and 12 mM calcium chloride, pH 9, at 37°C.

Spectroscopy. *Absorption spectra.* All absorption measurements were made with a Shimadzu model UV 160U spectrophotometer at room temperature.

The publication costs of this article were defrayed in part by page charge payment. This article must therefore be hereby marked "*advertisement*" in accordance with 18 U.S.C. §1734 solely to indicate this fact.

Fluorometry. All fluorescence measurements were carried out at 37°C with an SLM Aminco (Urbana, IL) model 48000 S spectrofluorometer. Excitation was with a xenon arc lamp through a monochromator set at 552 nm and a polarizer at 54.7° to the vertical (the magic angle). For time-based data acquisition, the emission was observed with the monochromator set at 580 nm through a vertical polarizer. For emission spectra, the same conditions were used except the emission monochromator was scanned from 565 to 650 nm, whereas for excitation spectra the emission monochromator was set at 580 nm and the excitation was scanned from 450 to 570 nm. Both monochromators had a resolution of 4-nm full-width at half maximum.

Cell Culture and Fluorescence Microscopy. The human promyelocytic leukemic cell line HL-60 was grown in RPMI medium 1640 containing 10% fetal calf serum. A single cell suspension was incubated with D-NorFES-D (1×10^{-7} M) and examined under a Zeiss Axioplan microscope with Nomarski and fluorescence optics. For the latter, standard rhodamine filters were used.

RESULTS AND DISCUSSION

The objective of the current work was to incorporate geometric constraints to allow H-type dimer formation into a new design for substrates to detect protease activities in biological samples such as blood and whole cells.

As a first step, a relatively rigid, bent polypeptide containing an amino acid sequence similar to that found at the cleavage site of the naturally occurring protease inhibitor α_1-antitrypsin was synthesized. This undecapeptide, whose sequence is DAIPN|SIPKGY (named NorFES), was then covalently derivatized with one tetramethylrhodamine (D) on each side of the cleavage site (D-NorFES-D). The presence of prolines between the cleavage site and each dye was intended to provide conformational constraints on the peptide backbone. Proximity and spatial orientation of the two fluorophores resulted in the quenching of 90% of the fluorescence in this substrate.

Upon addition of the serine protease elastase, which can recognize the cleavage sequence in NorFES, an increase in fluorescence intensity was monitored as a measure of protease activity (Fig. 1*a*) and, as shown in Fig. 1*b*, the wavelength emission maximum remained constant. (Addition of elastase to an equimolar mixture of singly labeled NorFES peptides, i.e., D-NorFES and NorFES-D, did not produce changes in either the fluorescence intensity or the wavelength.)

When the absorption spectra of the pre- and postcleaved D-NorFES-D solution (Fig. 2) were examined, a large change in the spectral shape was observed. The blue-shifted peak indicated a bichromophoric interaction in the intact peptide, suggesting the formation of intramolecular ground-state dimers. Intermolecular ground-state complexes between dyes on different polypeptides were ruled out by the finding that Beer's law was observed up to 5-fold excess of the concentration used here.

The spectral characteristics of ground-state dimers, which have previously been observed in solutions containing high ($>10^{-5}$ M) concentrations of xanthene dyes (7–9), or doubly labeled alkyl chains (10), or multiply labeled proteins (11–13), have been discussed in terms of exciton theory (6). This theory presents a framework for considering resonance interactions between individual dyes in loosely bound molecular aggregates. Exciton theory predicts that the doubly degenerate excited energy level in a system of two noninteracting monomers splits into two upon dimerization. In the Simpson–Peterson model of strong exciton coupling, this splitting between excited energy levels (2U) is considered to be significantly greater than the Franck–Condon bandwidth ($\Delta\varepsilon$) of the

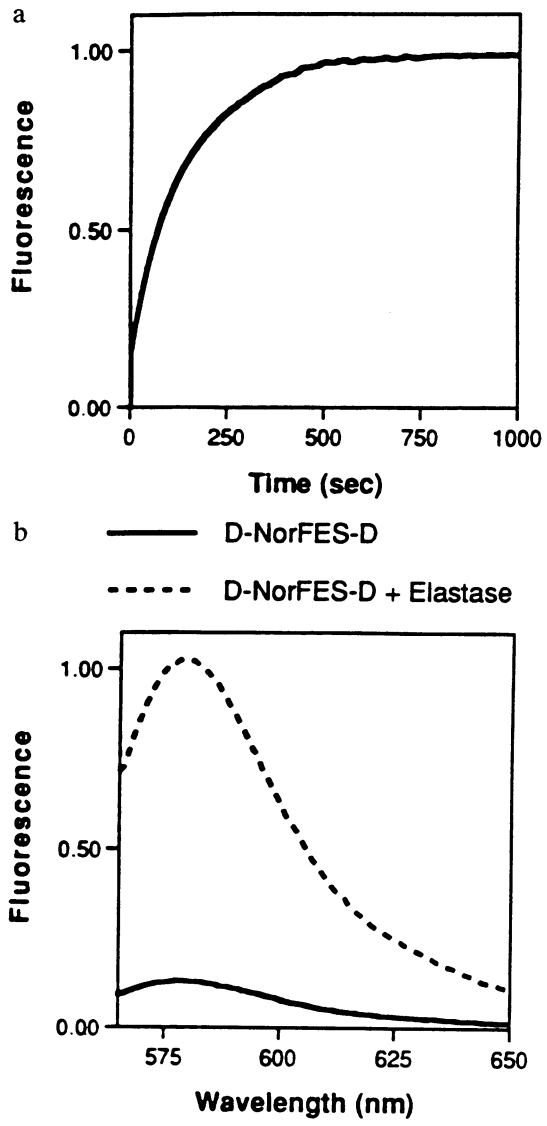

FIG. 1. (*a*) Fluorescence as a function of time after addition of the serine protease elastase. (*b*) Emission spectra of D-NorFES-D before (solid curve) and after (dashed curve) addition of elastase.

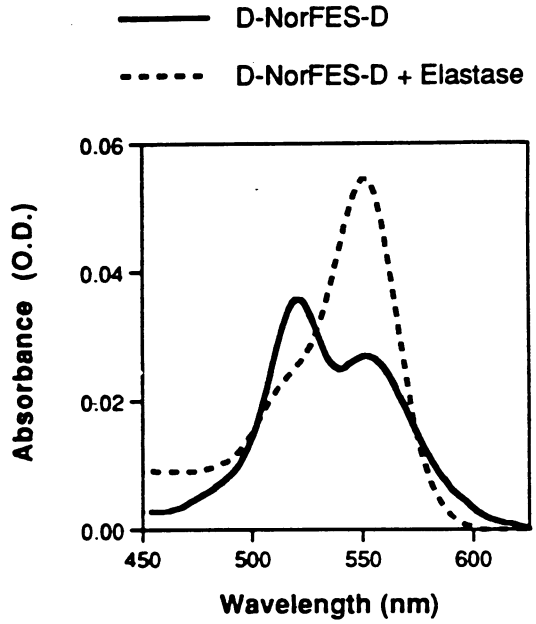

FIG. 2. Absorption spectra of D-NorFES-D before (solid curve) and after (dashed curve) addition of elastase.

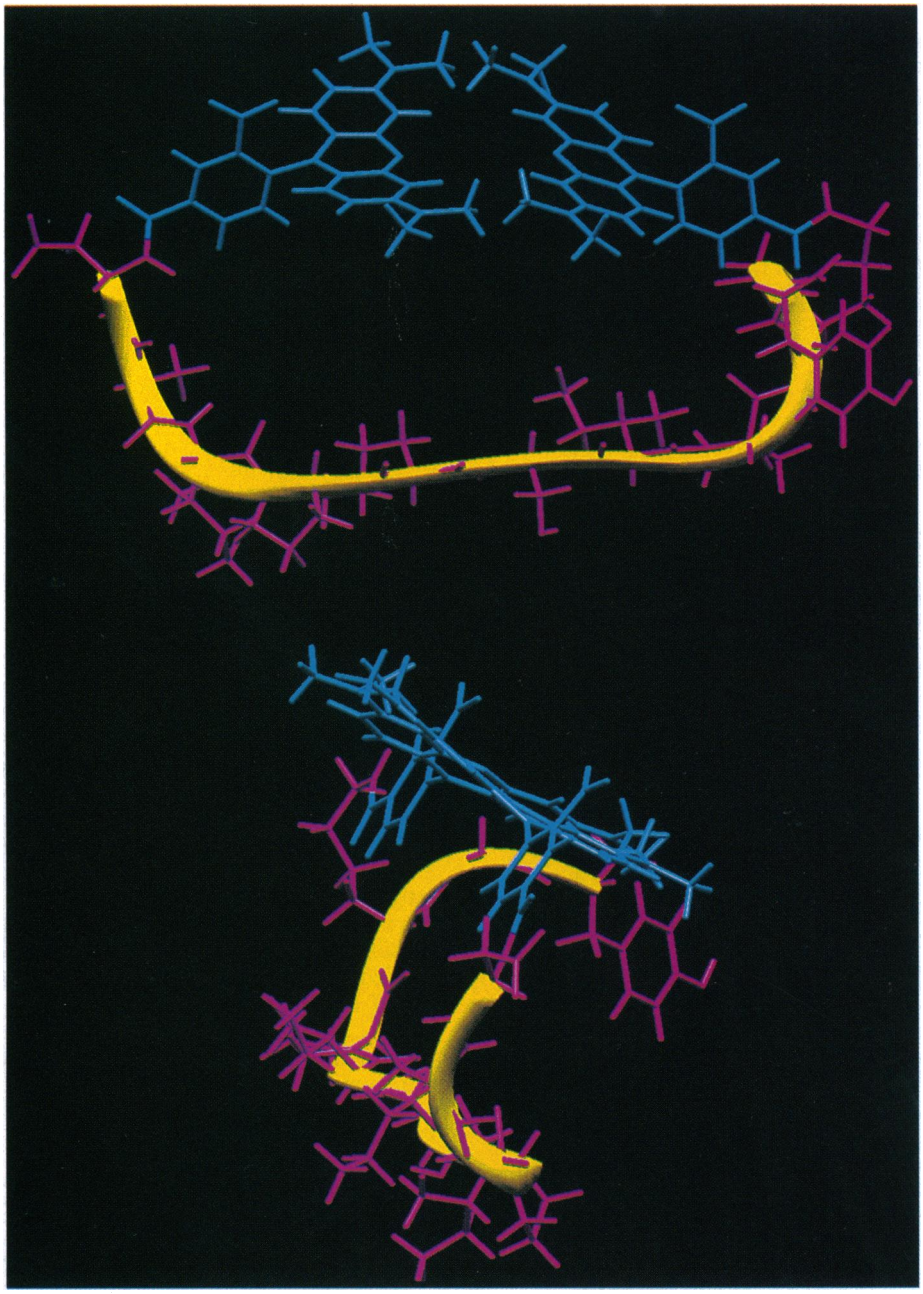

FIG. 3. Illustration of D-NorFES-D. The representation from two angles is based on information available from spectroscopic data. Dimer formation is accompanied by a blue-shift of the 552 nm band and a red-shift of the 353 nm band. Both transition dipoles are parallel to the plane of the three-ring system of each fluorophore with the 552 mn dipole being parallel and the 353 nm dipole perpendicular to the nitrogen–nitrogen line. The magnitude of the spectral shift in the 552 nm band suggests a dipole–dipole distance of *ca.* 6 Å. The yellow ribbon represents the peptide backbone, the magenta color the amino acids, and the cyan the fluorophores.

corresponding molecular electronic levels in the individual molecular unit, i.e., $2U/\Delta\varepsilon \gg 1$ (14). Accordingly, if transitions from the ground level to both excited levels were allowed for each orientation of the monomers relative to each other, one would expect to see two absorption peaks positioned at plus and minus U/hc cm^{-1} from the major absorption peak of the monomer. However, if only a blue-shifted peak is observed, this is indicative of an H-type geometry, in which the transition dipoles in individual dyes are parallel to each other and normal to the radius vector connecting the two dyes. In contrast, the presence of only a red-shifted peak is indicative of the J-type geometry, in which both transition dipoles are parallel to the radius vector.

In the system under study, U/hc equals 1200 cm^{-1} and $\Delta\varepsilon$/hc is *ca.* 1500 cm^{-1}. Therefore, the conditions for applying the strong exciton coupling model of Simpson and Peterson are not absolutely satisfied; however, blue and red shifts are still indicative of H- and J-type dimers, respectively. Predicting the exact shape of the dimeric absorption spectrum would require a model that takes into consideration the actual value of $\Delta\varepsilon$.

Rhodamine dyes have two major electronic transitions in the visible and near UV ranges. The transition dipole corresponding to the 552 nm band is oriented along the nitrogen–nitrogen axis, whereas the one corresponding to the 353 nm band is also parallel to the plane of the three-ring system, but perpendicular to the nitrogen–nitrogen line. Thus, the presence of a blue shift of the 552 nm band together with a red shift of the 353 nm band in the absorption spectrum of intact D-NorFES-D suggests a parallel, side-by-side alignment of the two fluorophores in the elastase substrate (Fig. 3). An alternative struc-

ture would have the two rhodamines stacked on each other rather than the edge-on arrangement depicted in Fig. 3; however, there are at least two pieces of evidence against this alternative. First, one would expect to see blue shifts of both the 552 and 353 bands. Second, the stacked arrangement would most certainly be hydrophobically driven. Thus, replacement of rhodamines with more hydrophobic dyes, e.g., fluorescein or pyrene, should also result in stacked structures. However, when NorFES was doubly labeled with either fluorescein or pyrene, the absence of wavelength shifts in the absorption spectra indicated that ground-state dimers were not formed. (In addition, excimer formation in NorFES doubly labeled with pyrene was not observed.) Therefore, hydrophobic forces can only play a minor role in the formation of rhodamine dimers, which decreases the likelihood of a stacked configuration.

The distance (R) between the centers of the point-dipole systems was determined by using the Simpson–Peterson approximation in which the magnitude of the spectral shift (U/hc) is related to R by the following equation:

$$U = \frac{|d|^2}{n^2 \times R^3} \times |\kappa|, \quad [1]$$

where $|d|^2$ is the squared module of the transition dipole, n is the solvent refractive index (n = 1.333 in water), κ is the orientation factor,

$$\kappa = \cos\theta_{12} - 3\times\cos\theta_{1R} \times \cos\theta_{2R}, \quad [2]$$

and θ_{12}, θ_{1R}, and θ_{2R} represent the angles between the transition dipoles in dyes 1 and 2, between dipole 1 and the radius-vector R connecting the two dipoles, and between dipole 2 and the radius-vector R, respectively. In the case of H-dimers $\theta_{12} = 0$, $\theta_{1R} = \theta_{2R} = 90°$, which yields $\kappa = 1$. The value of U/hc for D-NorFES-D obtained from the absorption peak shift equals 1200 cm^{-1}, which gives $U = 2.4 \times 10^{-13}$ erg, and the value of $|d|^2$, calculated by integrating under the main absorbance band in the rhodamine monomer, is equal to 1.0×10^{-34} erg·cm^3. Substituting these values in Eq. **1** gives the value of $R = 6.1 \times 10^{-8}$ cm. The structure depicted in Fig. 3 is based on this distance.

As shown in Fig. 1*b*, the fluorescence intensity of the solution containing the intact D-NorFES-D was 10% of that of the fully cleaved peptide. To compare the relative fluorescence of the monomer and dimer, excitation and absorption spectra were taken of the intact doubly labeled substrate. As shown in Fig. 4, the corrected excitation spectrum superimposed on the absorption spectrum points to a fluorescent monomer and nonfluorescent dimer. In fact, the excitation spectrum closely resembles the absorption spectrum of the monomer, and, therefore, the 10% of fluorescence intensity observed in the precleaved peptide solution is probably coming from the monomers that did not form dimers. [Additional synthetic analogs indicate modification to the peptide backbone can result in an increase in the dimer to monomer ratio (unpublished work)]. This is also consistent with the fact that emission spectra of identical shape were produced by the pre- and postcleaved D-NorFES-D, irrespective of whether the excitation was at 518 or 552 nm (the absorption peaks of the dimer and monomer, respectively). The absence of fluorescence is characteristic of H-type dimers where radiative transitions between the ground and lowest excited states are forbidden and the electronic excitation energy is lost via a nonradiative channel.

The radiative rate for the transition from the lowest excited state of the dimer to the ground state (k_r^d) is given by the following expression:

$$k_r^d = k_r^m \times [1 - (\text{sign}\kappa) \times \cos\theta_{12}], \quad [3]$$

where k_r^m is the radiative rate of the monomer, (sign κ) = +1 when $\kappa > 0$, (sign κ) = −1 when $\kappa < 0$, and (sign κ) = 0 when $\kappa = 0$ (in the latter case no characteristics of dye interactions are observable). Since the accuracy of our measurements was *ca.* 1%, the value of k_r^d does not exceed 1% the value of k_r^m. Assuming $\kappa > 0$, Eq. **3** gives the upper limit for θ_{12} as 8°.

If the dimer were fluorescent, then valuable information about its geometry could be obtained from fluorescence anisotropy data. Therefore, in order to assess the source of the residual 10% fluorescence of D-NorFES-D, we measured the anisotropy of D-NorFES-D in aqueous solution and in 90% glycerol. In the former, the anisotropy value is close to zero due to the fast tumbling of this small molecule. In the latter, the formation of dimers was not observed, a finding that can be related to the lower polarity of glycerol (ε = 42) as compared with water (ε = 80): the repulsion of like charges in glycerol is stronger and this prevents the two dyes from forming a dimer.

Profluorescent peptide protease detection reagents used in the past have also contained two fluorophores, one on each side of the cleavage site (15, 16). However, in contrast to the design presented in the present work where the two dyes are identical, the prior work used peptides with two different, but spectroscopically complimentary, probes (*vide infra*). Thus, dequenching of these heterolabeled substrates by active proteases has usually been ascribed to the loss of a Förster type of energy transfer (17–20) in which one would expect cleavage to result in an increase in emission intensity of the donor and a decrease in emission wavelength maximum but no absorption differences. Therefore, to determine if the exciton mechanism might be operational in a heterolabeled substrate, NorFES was labeled with tetramethylrhodamine (D) on one side of the cleavage site and rhodamine-X (A) on the other. (Both D-NorFES-A and A-NorFES-D were synthesized and gave similar results.) D and A are spectroscopically related by virtue of the emission of the former overlapping with the excitation of the latter. As expected, upon addition of the protease, the fluorescence intensity increased and the emission peak wavelength decreased (by *ca.* 13 nm).

Most critical for the question at hand was to compare (*i*) the absorption spectra of the pre- and postcleaved heterodoubly labeled substrates and (*ii*) the absorption and excitation spectra of the precleaved molecule. First, the blue-shift in the

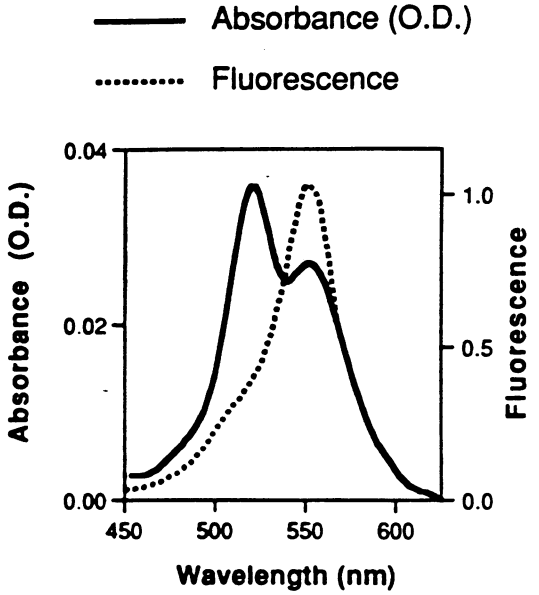

FIG. 4. Superposition of absorption (solid curve) and excitation (dotted curve) spectra of D-NorFES-D.

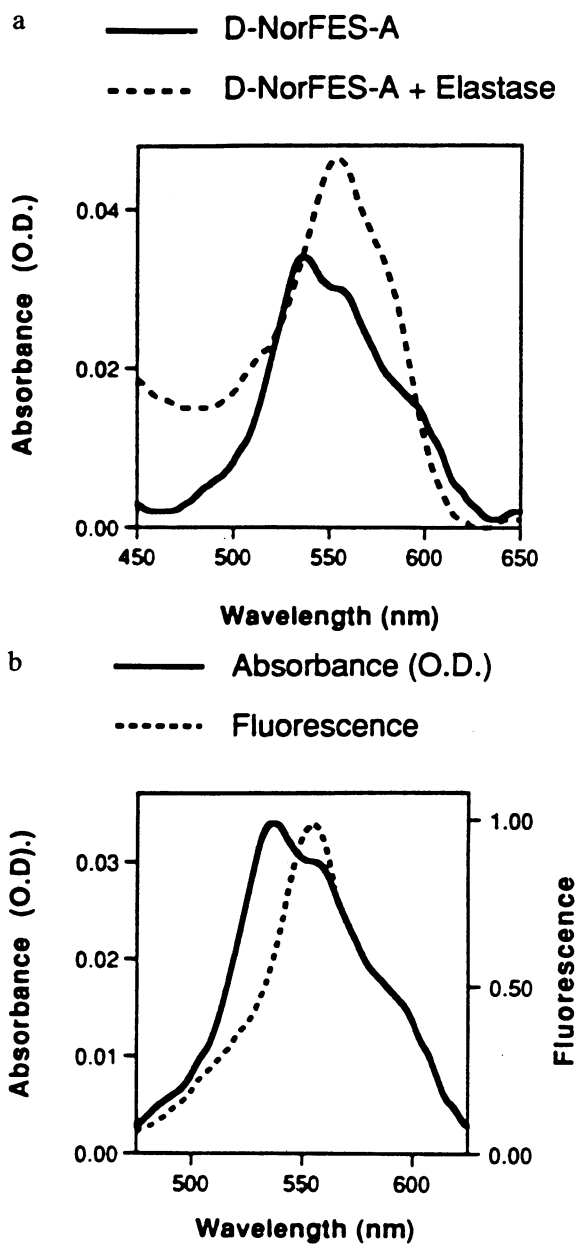

FIG. 5. (*a*) Absorption spectra of D-NorFES-A (tetramethylrhodamine-DAIPN$_i$SIPK-(ε-rhodamine-X)-GY before (solid curve) and after (dashed curve) addition of 1 unit of elastase. (*b*) Superposition of absorption (solid curve) and excitation (dotted curve) spectra of D-NorFES-A.

maximum of the absorption spectrum of D-NorFES-A compared with the spectrum after enzymatic digestion of the peptide (Fig. 5*a*) is inconsistent with the Förster mechanism; rather, it is suggestive of an exciton splitting similar to that described above. Second, the superposed composite of the absorption and excitation spectra (Fig. 5*b*) indicates that all of the fluorescence is from the two monomeric fluorophores, as is the case with D-NorFES-D. Additionally, Förster energy transfer, which can be considered to be a localization of excitons, may occur only when the electronic energy gap between two dyes substantially exceeds the energy of the dipole–dipole interaction (U). The energy gap between D and D equals zero and that between D and A equals 875 cm^{-1}; U/hc is estimated to be *ca.* 1200 cm^{-1} for both systems. Therefore, in neither the homolabeled nor the heterolabeled case is localization possible; this makes both sets of data consistent with an exciton mechanism.

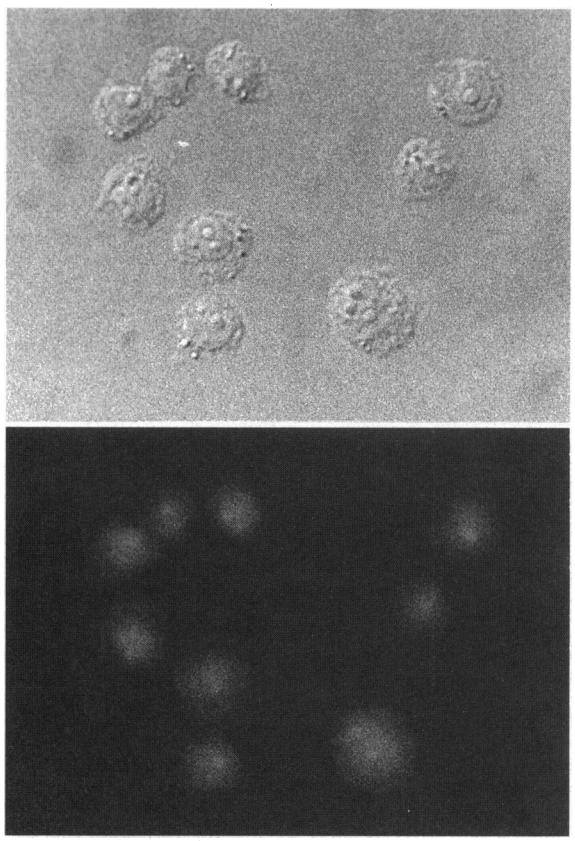

FIG. 6. HL-60 cells after addition of D-NorFES-D (1×10^{-7} M) as viewed under (*a*) Nomarski and (*b*) fluorescence optics (×2640).

Based on the above biophysical results, the biological application described below appeared feasible. Although a heterodoubly labeled substrate can serve as a probe for protease activity if an interference filter with a narrow bandpass is used on the emission side of a sample (the emission from the acceptor must be blocked), use of a homodoubly labeled peptide would only require an emission filter that blocked out the excitation light. Since standard optics on the emission side of fluorescence microscopes include only a barrier filter that blocks light below a specific wavelength, D-NorFES-A would be of little value in this setting. In contrast, the quenching of a single type of fluorophore in H-type dimers, as in D-NorFES-D, makes this protease probe compatible with all fluorescence microscopes. Using the principle of excitons, the intracellular elastase activity of the promyelocytic leukemic cells of the HL-60 line was visualized with D-NorFES-D (Fig. 6). This application has the potential for significant advancement in enzymology since in the past intracellular protease molecules have only been observed using labeled antibodies and, unfortunately, most proteases exist in a proactive or latent form. Therefore, the mere presence of a protease molecule does not necessarily correlate with biological activity. Thus, since the excitons in intramolecular dimers presented here do not decay radiatively and fluorescence appears only in the presence of proteolytic activity, this substrate design allows *in situ* protease activity detection. Insights into physiological and pathological processes where protease activities are believed to play significant roles, e.g., tissue remodeling, inflammation, and cancer metastasis, become possible.

In conclusion, synthesis and spectroscopic analysis of two doubly labeled peptide protease substrates, one of which was homolabeled and the other heterolabeled, provides the basis for a new class of protease substrates, i.e., intramolecular H-type dimers. The significance of this work may lie in the design of improved molecular probes for enzymatic as well as

dynamic conformational analysis for many classes of macromolecules. In view of the current importance of protease inhibitor drug design, the addition of a new technique for dynamic conformational analysis, particularly of molecules which can modulate proteolytic activity at proteases' active sites, may become useful in the design of the next generation of protease inhibitors.

We gratefully acknowledge the assistance of Dr. Michael Rodgers and Andrew Russo with the computer graphics, Dr. S. Ayukawa for mass spectral analyses, and Dr. Wayne Kuenzel for use of the fluorescence microscope. The work was supported in part by National Institutes of Health Grant GM11632.

1. Kasha, M. (1991) in *Physical and Chemical Mechanisms in Molecular Radiation Biology*, eds. Glass, W. A. & Varma, M. N. (Plenum, New York), pp. 231–255.
2. Davydov, A. S. (1962) *Theory of Molecular Excitons* (McGraw-Hill, New York).
3. Hochstrasser, R. M. & Kasha, M. (1964) *Photochem. Photobiol.* **3,** 317–331.
4. Kasha, M., Rawls, H. R. & Ashraf El-Bayoumi, M. (1965) *Pure Appl. Chem.* **2,** 371–392.
5. Kasha, M. (1963) *Radiat. Res.* **20,** 55–71.
6. Valdes-Aguilera, O. & Neckers, D. C. (1989) *Acc. Chem. Res.* **22,** 171–177.
7. Förster, T. & König, E. (1957) *Ber. Bunsenges. Phys. Chem.* **61,** 344–348.
8. Selwyn, J. E. & Steinfeld, J. I. (1972) *J. Phys. Chem.* **76,** 762–774.
9. Arbeloa, I. L. & Ojeda, P. R. (1982) *Chem. Phys. Lett.* **87,** 556–560.
10. Luttrull, D. K., Valdes-Aguilera, O., Linden, S. M., Paczkowski, J. & Neckers, D. C. (1988) *Photochem. Photobiol.* **47,** 551–557.
11. Ravdin, P. & Axelrod, D. (1977) *Anal. Biochem.* **80,** 585–592.
12. Ajtai, K., Ilich, P. J. K., Ringler, A., Sedarous, S. S., Toft, D. J. & Burghardt, T. P. (1992) *Biochemistry* **31,** 12431–12440.
13. Hamman, B. D., Oleinikov, A. V., Jokhadze, G. G., Bochkariov, D. E., Traut, R. R. & Jameson, D. M. (1996) *J. Biol. Chem.* **271,** 7568–7573.
14. Simpson, W. T. & Peterson, D. L. (1957) *J. Chem. Phys.* **26,** 588–593.
15. Latt, S. A., Auld, D. S. & Vallee, B. L. (1972) *Anal. Biochem.* **50,** 56–62.
16. Carmel, A., Zur, M., Yaron, A. & Katchalski, E. (1973) *FEBS Lett.* **30,** 11–13.
17. Wu, P. & Brand, L. (1994) *Anal. Biochem.* **218,** 1–13.
18. VanDer Meer, B. W., Coker, G., III & Chem, S.-Y. S. (1994) *Resonance Energy Transfer, Theory and Data* (VCH, New York).
19. Selvin, P. (1995) *Methods Enzymol.* **246,** 300–334.
20. Clegg, R. M. (1995) *Curr. Opin. Biotechnol.* **6,** 103–110.